


SCIENTIFIC REPORTS

OPEN

Combination of eribulin plus AKT inhibitor evokes synergistic cytotoxicity in soft tissue sarcoma cells

Naotaka Hayasaka¹, Kohichi Takada^{1,2}, Hajime Nakamura¹, Yohei Arihara¹, Yutaka Kawano¹, Takahiro Osuga¹, Kazuyuki Murase^{1,2}, Shohei Kikuchi^{1,2}, Satoshi Iyama², Makoto Emori³, Shintaro Sugita⁴, Tadashi Hasegawa⁴, Akira Takasawa⁵, Koji Miyanishi¹, Masayoshi Kobune¹  & Junji Kato¹

An activated AKT pathway underlies the pathogenesis of soft tissue sarcoma (STS), with over-expressed phosphorylated AKT (p-AKT) correlating with a poor prognosis in a subset of STS cases. Recently, eribulin, a microtubule dynamics inhibitor, has demonstrated efficacy and is approved in patients with advanced/metastatic liposarcoma and breast cancer. However, mechanisms of eribulin resistance and/or insensitivity remain largely unknown. In this study, we demonstrated that an increased p-AKT level was associated with eribulin resistance in STS cells. We found a combination of eribulin with the AKT inhibitor, MK-2206, synergistically inhibited STS cell growth *in vivo* as well as *in vitro*. Mechanistically, eribulin plus MK-2206 induced G1 or G2/M arrest by down-regulating cyclin-dependent kinases, cyclins and cdc2, followed by caspase-dependent apoptosis in STS cells. Our findings demonstrate the significance of p-AKT signaling for eribulin-resistance in STS cells and provide a rationale for the development of an AKT inhibitor in combination with eribulin to treat patients with STS.

Soft tissue sarcoma (STS) originating from mesenchymal cells is a rare neoplasm that accounts for around 1% of all adult malignancies¹. STS comprise a heterogeneous group of over 50 recognized histological subtypes². The prognosis for unresectable or metastatic (UM)-STS cases is poor, with an overall survival (OS) of less than 1.2 years after diagnosis³. Recommended therapy for most patients with UM-STs is doxorubicin (Dox), a first-line palliative chemotherapy used for over 40 years⁴. Recently, three new drugs, pazopanib⁵, trabectedin⁶ and eribulin⁷, have been introduced for the treatment of UM-STs after Dox therapy. In 2016, eribulin was approved for patients with UM-STs who were previously treated with an anthracycline-containing regimen⁷. Eribulin is a novel microtubule dynamics inhibitor that is a modified analog of halichondrin B⁸. Remarkably, of the three novel therapeutics, only eribulin significantly improved OS compared to dacarbazine. However, outcomes with eribulin for UM-STs may not be enough to fully address unmet clinical needs, in particular for relapsed patients. Therefore, despite the efficacy of eribulin in the disease, the prognosis of UM-STs remains difficult, and there is a need to further develop novel strategies for the treatment of this disease.

Generally, *de novo* and acquired resistances to anti-cancer drugs frequently arise that hamper the results of cancer therapy⁹. However, the mechanisms of eribulin resistance have been largely unknown. Exploring the mechanisms of resistance to eribulin may lead to creating new treatment strategies for UM-STs.

The protein serine/threonine kinase, AKT, also termed protein kinase B, is a pivotal regulator of numerous cellular processes including apoptosis, survival, proliferation and metabolism¹⁰. Overexpressed p-AKT underlies the pathogenesis of a broad range of human malignancies, including STS, such as leiomyosarcoma, fibrosarcoma, liposarcoma and undifferentiated pleomorphic sarcoma^{2,11–13}. Of note, the high expression of p-AKT has been

¹Department of Medical Oncology, Sapporo Medical University School of Medicine, Sapporo, Japan. ²Department of Hematology, Sapporo Medical University School of Medicine, Sapporo, Japan. ³Department of Orthopedic Surgery, Sapporo Medical University School of Medicine, Sapporo, Japan. ⁴Department of Surgical Pathology, Sapporo Medical University School of Medicine, Sapporo, Japan. ⁵Department of Molecular and Cellular Pathology, Sapporo Medical University School of Medicine, Sapporo, Japan. Naotaka Hayasaka and Kohichi Takada contributed equally. Correspondence and requests for materials should be addressed to K.T. (email: ktakada@sapmed.ac.jp)

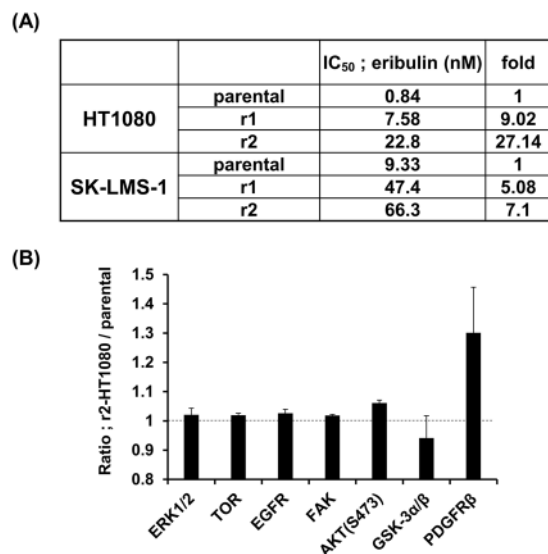


Figure 1. Eribulin resistance in STS cells is associated with up-regulated p-AKT. (A) STS cell lines, including eribulin-resistant cell lines (r1 and r2), were cultured in the presence of eribulin for 48 h. Cell proliferation was assessed in triplicate cultures by 3-(4,5-dimethylthiazol-2-yl)-2,5-diphenyl tetrazolium bromide (MTT) assay. The IC₅₀ values shown refer to growth inhibition by eribulin. The experiments were repeated three times. (B) Immunoblots of protein extracts from parental (HT1080) and r2-HT1080 cell lines were obtained. The phosphorylation status of a panel of proteins was evaluated by image analyzer. The data represents a comparison of parental HT1080 and r2-HT1080 cell lines.

identified as a negative surrogate marker for the survival of patients with STS. Therefore, AKT may represent an attractive target for STS therapeutics.

In the current study, we performed phospho-protein arrays with HT1080 and eribulin resistant HT1080 cell lines to investigate the molecular mechanisms of eribulin resistance in STS cells. This assay revealed that p-AKT levels were up-regulated by eribulin treatment. These observations prompted us to assess the cytotoxicity of eribulin plus AKT inhibitor and whether this combination treatment can overcome eribulin resistance in STS cells. A combination of the AKT inhibitor, MK-2206, with eribulin resulted in synergistically induced G1 or G2/M arrest, followed by apoptosis in STS cells. Overall, our findings provide a clinical framework for using MK-2206 with eribulin to treat patients with UM-STs.

Results

Over-expressed p-AKT is associated with eribulin resistance. To establish stable STS cell lines with resistance to eribulin, HT1080 (fibrosarcoma) and SK-LMS-1 (leiomyosarcoma) cells were exposed to increasing concentrations of eribulin. Resistant cell lines derived from these cell lines were termed r1/r2-HT1080 and r1/r2-SK-LMS-1, respectively. The resistance of these cells to eribulin compared to parental cells was evaluated with 3-(4,5-dimethylthiazol-2-yl)-2,5-diphenyl tetrazolium bromide (MTT) assays. The IC₅₀ values of resistant cells were from 5.08- to 27.14 -fold greater than in the parental cells (Fig. 1A).

Growing evidence suggested oncogenes, tumor suppressor genes, and transporter pumps are linked to chemoresistance in numerous cancers⁹. In particular, the activation of oncogenes, such as *PI3K/AKT*⁹, *ERK*¹⁴, *NF-κB*¹⁵, *EGFR*¹⁶ and *PDGFR-β*¹⁷, by phosphorylation induced chemoresistance in cancer cells. However, mechanisms of eribulin resistance are less well studied in STS cells. First, we directed our efforts toward screening the phosphorylation status of a panel of kinases, known as oncogenes, using a phospho-kinase array. As shown in Fig. 1B, the expression of *PDGFR-β* and p-AKT(S473) was increased in r2-HT1080 cells compared to parental cells. This data refers to biological triplicates. We analyzed the result of an array to select druggable targets that can be promptly applied to clinical studies. First, we focused on *PDGFR-β*, since this is one of the targets of pazopanib, a drug that has already been introduced to patients with STS⁵. We carried out an MTT assay to analyze the cytotoxicity of eribulin plus pazopanib (Supplementary Fig. S1). Unfortunately, this combination did not trigger a synergistic effect in HT1080 cells. The change noted in p-AKT of r2-HT1080 cells was small. We also examined the expression of p-AKT(S473) protein levels in r1/r2-HT1080 and r1/r2-SK-LMS-1 cells by western blotting to confirm the array data. We observed the increased expression of p-AKT(S473) in all eribulin-resistant cell lines (Fig. 2A). Moreover, p-AKT levels were up-regulated, in a dose-dependent fashion, by eribulin treatment for 48 h in parental HT1080, SK-LMS-1 and SW872 (liposarcoma) cell lines (Fig. 2B). These results indicated that eribulin resistance in STS cells may be associated with the phosphorylation of AKT(S473) triggered by eribulin.

The combination of eribulin and MK-2206 triggers synergistic anti-sarcoma activity. Based on our results, we expected that a combination of eribulin plus AKT inhibitor would be effective therapy to overcome eribulin resistance in STS. We chose MK-2206 as an AKT inhibitor in this study since this is an allosteric and

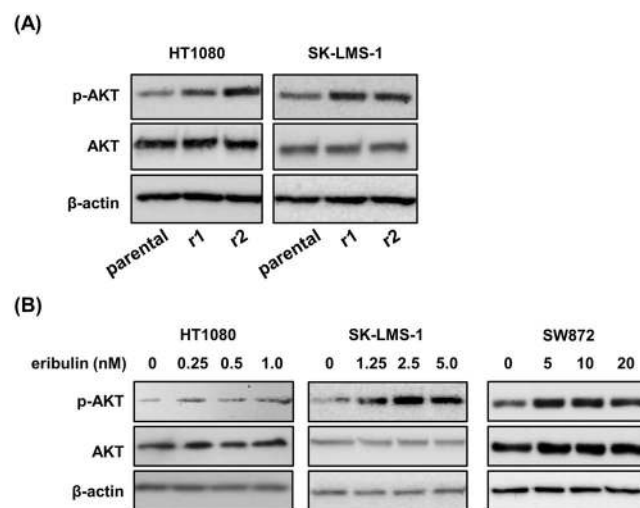


Figure 2. Eribulin treatment promotes phosphorylation of AKT in STS cells. **(A)** Immunoblot of total protein extracts obtained from parental and eribulin-resistant cell lines. The active form of AKT was analyzed using an anti-pAKT (S473) antibody. **(B)** STS cells were treated with increasing dosages of eribulin for 48 h. Whole cell lysates were subjected to immunoblotting using anti-p-AKT, AKT and β-actin antibodies. These experiments were repeated three times.

highly selective inhibitor¹⁸, and has been evaluated in several clinical trials^{19–22}. Initially, we assessed the cytotoxicity of eribulin and MK-2206, respectively. Eribulin and MK-2206 suppressed the growth of STS cell lines, with values for IC_{50} shown for various cell lines (Fig. 3A,B). Subsequently, we conducted a study of combination treatment using an MTT assay to test whether MK-2206 with eribulin induced increased cytotoxicity compared with each monotherapy. A combination of eribulin plus MK-2206 induced synergistic cytotoxicity in parental STS cell lines at all indicated MK-2206 doses (Fig. 3C), accompanied by the inhibition of AKT phosphorylation (Supplementary Fig. S2). Even in cells resistant to eribulin, a subset of combination doses triggered synergistic cytotoxicity (Fig. 3D). Of note, eribulin plus MK-2206 treatment at IC_{50} values (Fig. 1A and Supplementary Table S1) suppressed cell growth in established STS cell lines with resistance to eribulin (Fig. 3D).

Eribulin plus MK-2206 promotes G1 or G2/M arrest in STS cells. To elucidate the cytotoxic mechanisms of eribulin plus MK-2206 in STS cells, we examined the effects of combination treatment on the cell cycle. HT1080 and SK-LMS-1 cell lines were treated with eribulin with or without MK-2206 IC_{25} concentrations, for 24 hours and analyzed by flow cytometry. Eribulin is known to induce G2/M arrest²³, while MK-2206 promotes G1 arrest in cancer cells¹⁸. As expected, eribulin significantly induced G2/M arrest in STS cells (Fig. 4A; $P < 0.01$), but its effect at the indicated concentrations in SK-LMS-1 cells was of a low power. MK-2206 treatment significantly increased the percentage of cells in the G1 phase and significantly decreased the percentage of cells in the S phase in both cell lines (Fig. 4A; $P < 0.05$ for HT1080 and $P < 0.01$ for SK-LMS-1). Notably, eribulin plus MK-2206 treatment dramatically induced G1 arrest in HT1080 cells, and G2/M arrest in SK-LMS-1 cells (Fig. 4A; $P < 0.01$ for both). To analyze the mechanism of G1 or G2/M arrest induced by eribulin plus MK-2206, we determined protein levels of several cell cycle-related proteins in STS cells using western blotting. The expression of the G1 arrest-associated proteins, CDK4/6 and cyclin D3, were apparently decreased, while p21 expression was increased (Fig. 4B). In terms of G2/M arrest, the expression of cdc2 and cyclin B1 was suppressed simultaneously. These results showed that combination treatment of eribulin plus the AKT inhibitor MK-2206 inhibited the proliferation of STS cells and this was accompanied by G1 or G2/M arrest with the down-regulation of CDK4/6, cdc2 and cyclin B1/D3.

Eribulin plus MK-2206 treatment induces caspase-dependent apoptosis. To investigate whether eribulin plus MK-2206 might also evoke apoptosis in STS cells, we performed flow cytometry analysis. As shown in Fig. 5B, Annexin V/7-AAD staining showed a remarkably higher percentage of apoptosis among HT1080 and SK-LMS-1 cells. Treatment with the pan-caspase inhibitor, Q-VD-OPH, inhibited eribulin plus MK-2206-induced apoptosis. We next assessed whether the apoptosis was mediated via an intrinsic or extrinsic pathway using flow cytometry. The activities of caspases 8 and 9 were significantly up-regulated by eribulin plus MK-2206 treatment compared to each monotherapy cohort (Fig. 5B). These data suggested that eribulin plus MK-2206-induced apoptosis occurred mediated through intrinsic and extrinsic caspase-dependent pathways. Taken together, this combination therapy may be effective for UM-STS patients in a clinical setting.

Anti-tumor effect of eribulin plus MK-2206 in STS xenograft models. To explore the clinical potential of eribulin plus MK-2206, we examined the ability of this combination therapy to inhibit STS tumor growth *in vivo* using a subcutaneous HT1080 murine xenograft model. Mice were treated with 0.25 mg/kg eribulin once a week in combination with, or without, 0.12 mg/kg MK-2206 three times per week for three weeks. Tumor burden was significantly suppressed by treatment with eribulin compared with vehicle, whereas mice treated with MK-2206 showed a progressive increase in tumor volume throughout the evaluation period (Fig. 6A,B). When

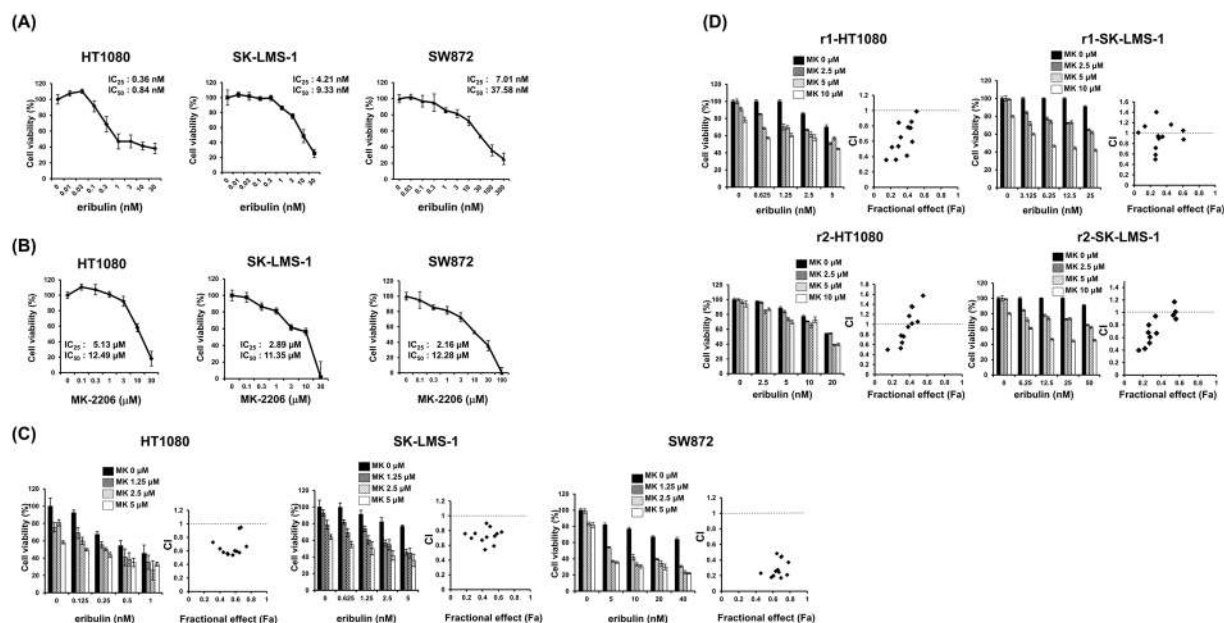


Figure 3. AKT inhibition by MK-2206 synergistically enhances eribulin-induced cytotoxicity in STS cells. (A,B) HT1080, SK-LMS-1 and SW872 cells were incubated with increasing doses of eribulin and MK-2206 for 48 h. Cell growth reduction was determined using 3-(4,5-dimethylthiazol-2-yl)-2,5-diphenyl tetrazolium bromide (MTT) assays. (C,D) HT1080, SK-LMS-1 and eribulin resistant cells (r1 and r2) were treated with or without the indicated concentrations of eribulin, MK-2206, or a combination of these for 48 h. The combination of eribulin plus MK-2206 induced synergistic cytotoxicity in even resistant cell lines, although this was less effective than in parental cell lines. The data represents the mean of four independent cultures. Error bars represent the standard deviation (SD). CI: Combination index. CI < 1: synergistic.

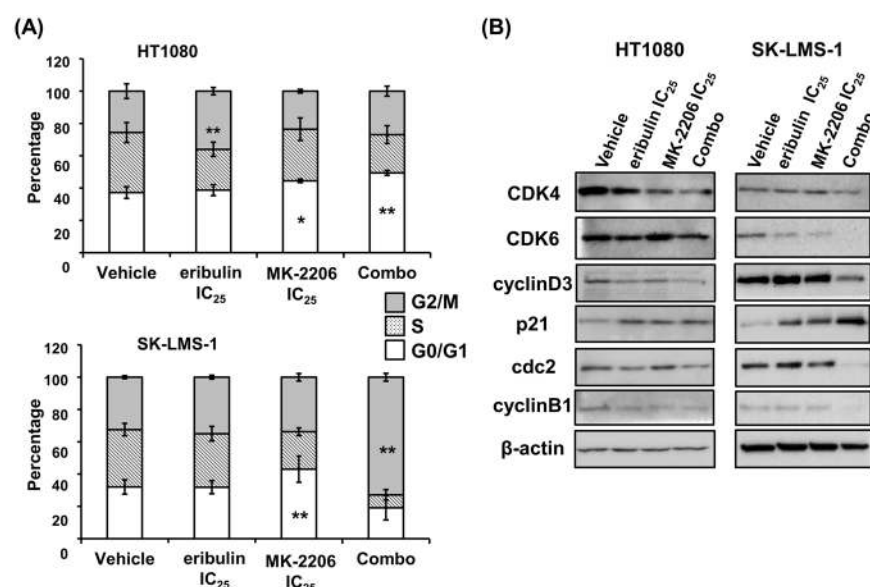


Figure 4. Combined treatment of eribulin plus MK-2206 triggers G1 or G2/M arrest in STS cells. (A) HT1080 or SK-LMS-1 cells were untreated (vehicle) or treated with eribulin and/or MK-2206 for 24 h, and then stained with propidium iodide. Subsequently, cell cycles were analyzed by flow cytometry. Error bars represent the standard deviation (SD). **P* < 0.05, ***P* < 0.01. Combo: combined eribulin and MK-2206. (B) Immunoblot analysis of cell lysates after treatment of cells with combined eribulin and MK-2206 for 24 h. Cell cycle-regulated proteins were analyzed using the indicated antibodies. The β-actin protein served as a loading control for each experiment. Combo: combined eribulin and MK-2206. These experiments were repeated three times.

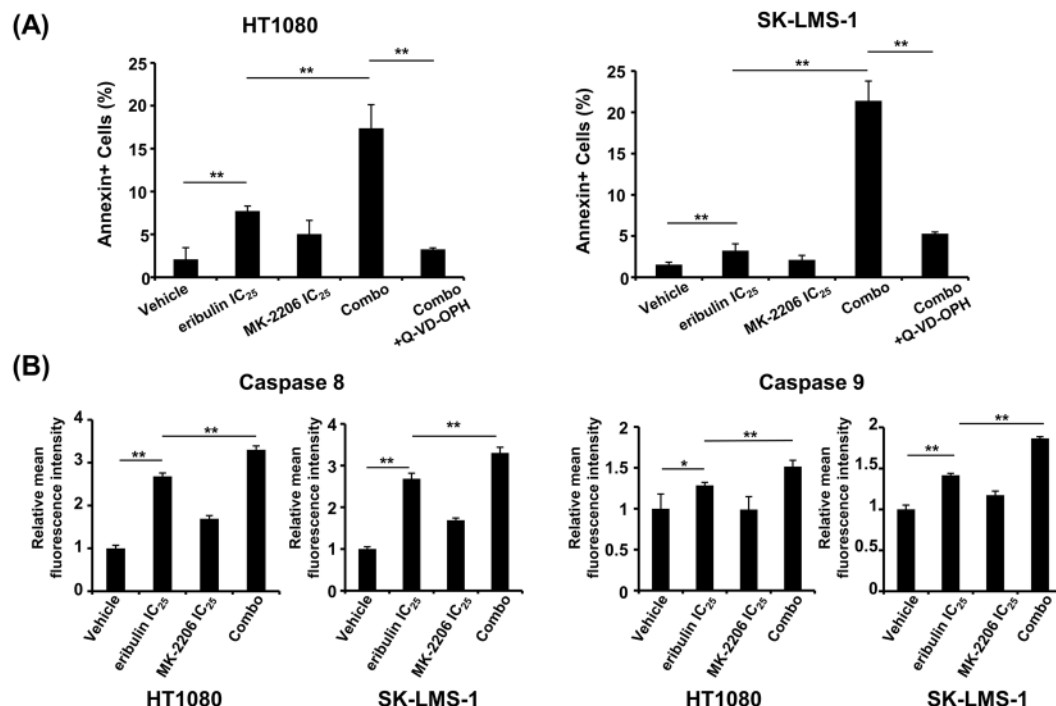


Figure 5. Combination treatment of eribulin plus MK-2206 induces caspase-dependent apoptosis of STS cells. **(A)** HT1080 and SK-LMS-1 cells were treated with IC₂₅ doses of eribulin, MK-2206, or a combination of both (combo), with or without a pan-caspase inhibitor, Q-VD-OPH (20 μ M), for 48 h. Q-VD-OPH was added 1 h before eribulin and MK-2206 treatments. Apoptotic cells were analyzed by flow cytometry using annexin V/7-AAD staining. Error bars represent the standard deviation (SD). ** $P < 0.01$. **(B)** HT1080 and SK-LMS-1 cells were treated with IC₂₅ doses of eribulin, MK-2206, or a combination of both (combo) for 48 h. Activities of caspases 8 and 9 were determined by flow cytometry. These experiments were repeated three times. Error bars represent the SD. * $P < 0.05$, ** $P < 0.01$.

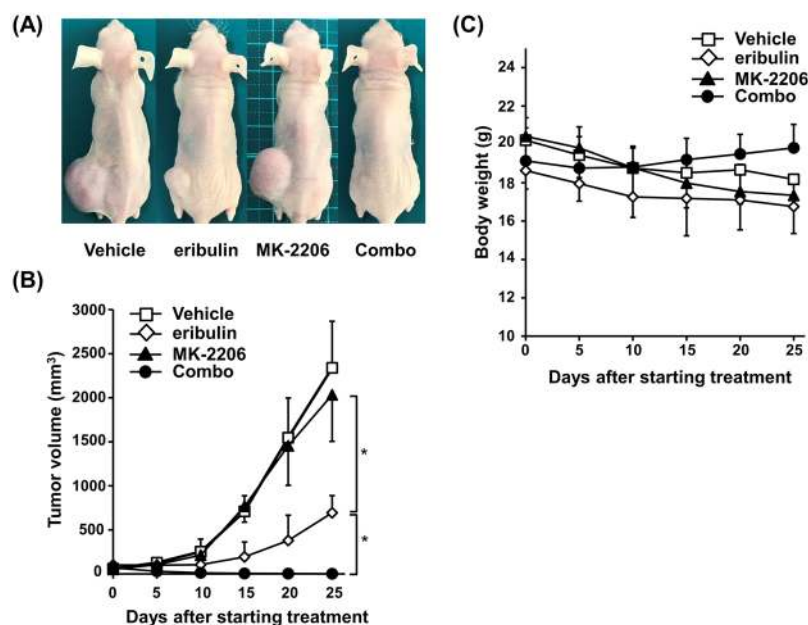


Figure 6. Combination of eribulin and MK-2206 augments tumor suppression in a mouse xenograft STS model. **(A)** Representative images of subcutaneous tumors in each group are shown. **(B)** Tumor volumes were measured and calculated at every treatment schedule. Data are presented as the mean of data \pm standard deviation (SD; $n = 5$). * $P < 0.01$. **(C)** Mice weights were monitored every 2 days. Data are presented as the mean of data \pm SD ($n = 5$). Combo: combined eribulin and MK-2206.

MK-2206 was administered in combination with eribulin, anti-tumor activity was dramatically enhanced as with *in vitro* studies. Strikingly, eribulin plus MK-2206 treatment led to complete responses in 4 of 5 mice, and was well tolerated, without causing significant body weight loss compared to the eribulin alone cohort in this experimental setting (Fig. 6C). No adverse effects in normal tissues were attributable to the administration of eribulin and/or MK-2206 upon necropsy during this study (data not shown). Collectively, these data suggested the possibility of applying this combination for UM-STs treatment.

Discussion

In the present study, our data demonstrated that AKT plays a key role in the resistance to eribulin by a subset of STS. These observations led us to evaluate combination therapy of eribulin with an AKT inhibitor to combat eribulin resistance and/or insensitivity in STS cells. Eribulin combined with MK-2206 dramatically inhibited STS cell growth *in vivo* as well as *in vitro*, suggesting its clinical application for patients with UM-STs whose prognosis is poor.

Eribulin is approved as a therapeutic for patients with UM-STs who have received a prior anthracycline-containing regimen, with liposarcoma as the indication in the United States and European Union²⁴. In Japan, eribulin can be used for all histological types of STS. A phase III trial revealed eribulin treatment significantly prolonged OS for 2 months compared to dacarbazine treatment for L-sarcoma⁷. To further evaluate efficacy in a relapsed/refractory setting, it was reasonable to explore combination therapy of eribulin with other agents. Additionally, identifying mechanisms of eribulin resistance may help in choosing agents to combine with eribulin. We hypothesize that AKT may be an appropriate target that can be applied promptly in clinical trials, with reference to the results of a phospho-kinase array and of previous reports^{19–22}. Therefore, we investigated the use of an AKT inhibitor in combination with eribulin to overcome eribulin resistance in STS cells. As expected, this combination therapy synergistically evoked cell-cycle arrest followed by apoptosis *in vitro*, and effectively exerted anti-tumor activity *in vivo* studies of STS cells. These proof-of-concept experiments highlight how eribulin plus an AKT inhibitor is a promising strategy for treating patients with UM-STs. Additionally, determining the expression level of p-AKT may be useful as a biological marker of eribulin responsiveness.

MK-2206 is a highly selective and orally active AKT inhibitor¹⁸. The efficacy and toxicity of MK-2206 for advanced solid tumors and hematological malignancies is under investigation in a clinical setting. A phase II study revealed that MK-2206 plus erlotinib was effective for advanced non-small cell lung cancer²⁰. In addition, two phase II studies for lymphoma and chronic lymphocytic leukemia, respectively, yielded favorable results^{19,21}. In terms of STS, one of three leiomyosarcoma patients showed stable disease for four months in a phase I study²². The doses of MK-2206 used in the current study were lower than those of previous studies in human cancers, which is encouraging for any future clinical trials.

It has been shown that breast cancer cells that harbor mutated *PTEN* or *PIK3CA* were sensitive to MK-2206²⁵. HT1080 and SK-LMS-1 cells that harbor wild-type *PTEN* and *PIK3CA* were resistant to MK-2206 in its clinical therapeutic ranges. Therefore, mutations of *PTEN* and *PIK3CA* may be related to sensitivity to MK-2206 in HT1080 and SK-LMS-1 cell lines. Accumulating evidence demonstrated MK-2206 increased the cytotoxicity of chemotherapeutics among a subset of cancer types, not only in experimental setups^{25,26} but in human studies also^{19,20,27}. To our knowledge, this study was the first attempt to find an effective eribulin-based therapy combined with other agents for STS. MK-2206 was found to sensitize cancer cells to DNA-damaging agents²⁸. Specifically, MK-2206 cytotoxicity was enhanced when combined with anti-microtubule inhibitors such as eribulin and paclitaxel²⁹. As previously reported, our present studies demonstrated that MK-2206 enhanced the eribulin-induced anti-tumor effect. Eribulin combined with MK-2206 induced G1 or G2/M arrest in STS cells. Such different mechanisms of cytotoxicity toward STS cells may depend on the cell type. Notably, this combination therapy evoked an extensive anti-tumor effect *in vivo* compared to *in vitro* studies. One of the plausible mechanisms for the drastic responses observed *in vivo* may be immune responses activated by eribulin treatment³⁰. However, further examination is required of eribulin in combination with MK-2206 in clinical studies of UM-STs patients.

In conclusion, this study demonstrated that activated AKT is associated with eribulin resistance in STS cells. Furthermore, eribulin in combination with MK-2206 synergistically suppresses STS growth through G1 or G2/M arrest, and, subsequently, caspase-dependent apoptosis. Our results highlight a potential clinical application for eribulin and MK-2206 combination therapy in the improvement of clinical outcomes in patients with UM-STs.

Materials and Methods

Reagents and human cell lines. Eribulin was kindly provided by Eisai Inc. (Tokyo, Japan) and Sapporo Medical University for *in vitro* and *in vivo* use, respectively. MK-2206 was obtained from ChemScene (Monmouth, NJ, USA). Pazopanib was obtained from AdooQ BioScience (Manassas, VA, USA). Stock solutions of these reagents were generated by dissolving the powder in 100% dimethyl sulfoxide (DMSO; Sigma–Aldrich St. Louis, MO, USA) at 10 mM. HT1080, SK-LMS-1 and SW872 cell lines were purchased from ATCC (Manassas, VA, USA). Both cell lines were maintained in DMEM (Sigma–Aldrich) containing 10% fetal bovine serum, 1% penicillin–streptomycin and 2 μ M L-glutamine.

Establishment of eribulin-resistant STS cell lines. Eribulin-resistant STS cell lines were generated by culturing HT1080 and SK-LMS-1 cell lines in stepwise increasing doses (0.1–5.0 nM and 1.0–10 μ M, respectively) of eribulin for more than 3 months. Resistant cell lines were named r1/r2-HT1080 and r1/r2-SK-LMS-1, and were continuously cultured in eribulin-containing media.

Phospho-kinase assay. Alterations in the phosphorylation status of multiple kinases in eribulin resistance compared to parental cells were screened using a Human Phospho-Kinase Array Kit (Proteome Profiler™ Array; R&D Systems, Minneapolis, MD, USA), which contained 43 different kinases. Briefly, cell lysates were prepared and incubated with membranes. Phosphorylated kinases were determined with an anti-phospho antibody. The

relative expressions of phosphorylated kinases were quantified with Image J software (Rasband, W.S., ImageJ, U.S. National Institutes of Health, Bethesda, Maryland, USA).

Cell cycle analysis. STS cells (5×10^5 /well) were incubated in medium containing eribulin and/or MK-2206 for 48 h. After collecting floating cells in media, adhesive cells were washed, fixed in ethanol, and stained with propidium iodide using a cell cycle analysis kit (FxCycle PI/RNase Staining Solution; Thermo Fisher Scientific, Waltham, MA, USA) according to the manufacturer's instructions, followed by analysis on a BD FACS Canto II instrument using FACSDiva. Cell cycle analysis was performed using Flow Jo software (Tree Star Inc.; Ashland, OR, USA).

Western blot analysis. As previously described³¹, cells were cultured with or without stimuli; cells were then harvested, washed, and lysed. Protein (40 µg) was denatured in SDS buffer and heated for 5 min at 100 °C. Proteins were separated on MULTIGEL II mini gels (COSMO BIO CO., LTD., Tokyo, Japan) and transferred to polyvinylidene fluoride membranes (Immobilon, Merck Millipore Ltd., Burlington, MA, USA). Membranes were blocked using 5% milk in phosphate buffered saline (PBS) for 30 min at RT and incubated overnight at 4 °C with primary antibodies: pAKT (#4058), AKT (#4685), cdk4 (#12790), cdk6(#13331), cyclinD3 (#2936), cyclinE1 (#4129), p21 (#2947), cdc2 (#9116), cyclinB1 (#4138; all from Cell Signaling Technology, Danvers, MA, USA); and actin-HRP (sc-1615; Santa Cruz Biotechnology, Dallas, TX, USA). After washing, stained proteins were visualized using LAS-4000 mini (Fujifilm, Tokyo, Japan).

Growth inhibition and apoptosis assays. The inhibitory effect of eribulin and MK-2206 on STS cell line growth was assessed by MTT assay. Apoptosis was quantified using an annexin V/7-AAD staining kit (Annexin V PE Apoptosis Detection Kit I; BD Biosciences, San Jose, CA, USA), followed by analysis on a BD FACS Canto II instrument using FACSDiva (BD Biosciences) as previously described³². Levels of caspases 8 and 9 were determined by flow cytometric assays using a caspase 8 assay kit (CaspasLux8-L1D2; OncoImmunit, Inc., Gaithersburg, MD, USA) and a caspase 9 assay kit (CaspasLux9-M1D2; OncoImmunit, Inc.), respectively.

Murine xenograft model of human STS. HT1080 cells were pelleted, resuspended in 100 µL of DMEM with 100 µL of Matrigel (Corning, Corning, NY, USA), and inoculated subcutaneously (5×10^5 cells per mouse) in the left flank into 5-week-old BALB/c-nu mice ($n = 5$ per cohort). When the tumor diameter reached 5 mm, mice were assigned to four cohorts that were treated with vehicle, MK-2206, or eribulin, with or without MK-2206. Eribulin (0.25 mg/kg) was injected once per week via tail vein, and MK-2206 (0.12 mg/kg), suspended in 30% Captisol was administered by oral gavage three times per week³³. Tumor volumes were calculated as previously reported³⁴. All animal studies were carried out in accordance with the National Institutes of Health guidelines for the use of laboratory animals. All animal protocols were conducted according to the protocol approved by the Animal Ethics Committee of the Sapporo Medical University School of Medicine. After completion of treatment, complete necropsy was performed to evaluate tumor suppressive and adverse effects in xenografts and normal tissues. Excised samples were subjected to hematoxylin and eosin staining.

Statistical analysis. Statistical significance of differences was determined using Student's *t* test or ANOVA and subsequent post-hoc tests when the multiple independent variables were compared. Statistical significance was defined as $P < 0.05$. Values for IC₂₅ and IC₅₀, and the combination index were calculated using CompuSyn software³⁵.

References

- Savina, M. *et al.* Patterns of care and outcomes of patients with METAstatic soft tissue SARcoma in a real-life setting: the METASARC observational study. *BMC Med* **15**, 78, <https://doi.org/10.1186/s12916-017-0831-7> (2017).
- Barretina, J. *et al.* Subtype-specific genomic alterations define new targets for soft-tissue sarcoma therapy. *Nat Genet* **42**, 715–721, <https://doi.org/10.1038/ng.619> (2010).
- Judson, I. *et al.* Doxorubicin alone versus intensified doxorubicin plus ifosfamide for first-line treatment of advanced or metastatic soft-tissue sarcoma: a randomised controlled phase 3 trial. *Lancet Oncol* **15**, 415–423, [https://doi.org/10.1016/S1470-2045\(14\)70063-4](https://doi.org/10.1016/S1470-2045(14)70063-4) (2014).
- Seddon, B. *et al.* Gemcitabine and docetaxel versus doxorubicin as first-line treatment in previously untreated advanced unresectable or metastatic soft-tissue sarcomas (GeDDiS): a randomised controlled phase 3 trial. *Lancet Oncol* **18**, 1397–1410, [https://doi.org/10.1016/S1470-2045\(17\)30622-8](https://doi.org/10.1016/S1470-2045(17)30622-8) (2017).
- van der Graaf, W. T. *et al.* Pazopanib for metastatic soft-tissue sarcoma (PALETTE): a randomised, double-blind, placebo-controlled phase 3 trial. *Lancet* **379**, 1879–1886, [https://doi.org/10.1016/S0140-6736\(12\)60651-5](https://doi.org/10.1016/S0140-6736(12)60651-5) (2012).
- Kawai, A. *et al.* Trabectedin monotherapy after standard chemotherapy versus best supportive care in patients with advanced, translocation-related sarcoma: a randomised, open-label, phase 2 study. *Lancet Oncol* **16**, 406–416, [https://doi.org/10.1016/S1470-2045\(15\)70098-7](https://doi.org/10.1016/S1470-2045(15)70098-7) (2015).
- Schoffski, P. *et al.* Eribulin versus dacarbazine in previously treated patients with advanced liposarcoma or leiomyosarcoma: a randomised, open-label, multicentre, phase 3 trial. *Lancet* **387**, 1629–1637, [https://doi.org/10.1016/S0140-6736\(15\)01283-0](https://doi.org/10.1016/S0140-6736(15)01283-0) (2016).
- Jordan, M. A. *et al.* The primary antimitotic mechanism of action of the synthetic halichondrin E7389 is suppression of microtubule growth. *Mol Cancer Ther* **4**, 1086–1095, <https://doi.org/10.1158/1535-7163.MCT-04-0345> (2005).
- Zheng, H. C. The molecular mechanisms of chemoresistance in cancers. *Oncotarget* **8**, 59950–59964, <https://doi.org/10.18632/oncotarget.19048> (2017).
- Manning, B. D. & Toker, A. AKT/PKB Signaling: Navigating the Network. *Cell* **169**, 381–405, <https://doi.org/10.1016/j.cell.2017.04.001> (2017).
- Setsu, N. *et al.* The Akt/mammalian target of rapamycin pathway is activated and associated with adverse prognosis in soft tissue leiomyosarcomas. *Cancer* **118**, 1637–1648, <https://doi.org/10.1002/ncr.26448> (2012).
- Lim, H. J., Wang, X., Crowe, P., Goldstein, D. & Yang, J. L. Targeting the PI3K/PTEN/AKT/mTOR Pathway in Treatment of Sarcoma Cell Lines. *Anticancer Res* **36**, 5765–5771, <https://doi.org/10.21873/anticancerres.11160> (2016).
- May, C. D. *et al.* Co-targeting PI3K, mTOR, and IGF1R with small molecule inhibitors for treating undifferentiated pleomorphic sarcoma. *Cancer Biol Ther* **18**, 816–826, <https://doi.org/10.1080/15384047.2017.1373230> (2017).

14. Liu, W. *et al.* HMGB1-mediated autophagy modulates sensitivity of colorectal cancer cells to oxaliplatin via MEK/ERK signaling pathway. *Cancer Biol Ther* **16**, 511–517, <https://doi.org/10.1080/15384047.2015.1017691> (2015).
15. Antoon, J. W. *et al.* Targeting NF κ B mediated breast cancer chemoresistance through selective inhibition of sphingosine kinase-2. *Cancer Biol Ther* **11**, 678–689 (2011).
16. Sette, G. *et al.* EGFR inhibition abrogates leiomyosarcoma cell chemoresistance through inactivation of survival pathways and impairment of CSC potential. *PLoS One* **7**, e46891, <https://doi.org/10.1371/journal.pone.0046891> (2012).
17. Meng, F. *et al.* PDGFR α and β play critical roles in mediating Foxq1-driven breast cancer stemness and chemoresistance. *Cancer Res* **75**, 584–593, <https://doi.org/10.1158/0008-5472.CAN-13-3029> (2015).
18. Hirai, H. *et al.* MK-2206, an allosteric Akt inhibitor, enhances antitumor efficacy by standard chemotherapeutic agents or molecular targeted drugs *in vitro* and *in vivo*. *Mol Cancer Ther* **9**, 1956–1967, <https://doi.org/10.1158/1535-7163.MCT-09-1012> (2010).
19. Larsen, J. T. *et al.* Akt inhibitor MK-2206 in combination with bendamustine and rituximab in relapsed or refractory chronic lymphocytic leukemia: Results from the N1087 alliance study. *Am J Hematol* **92**, 759–763, <https://doi.org/10.1002/ajh.24762> (2017).
20. Lara, P. N. *et al.* Phase II Study of the AKT Inhibitor MK-2206 plus Erlotinib in Patients with Advanced Non-Small Cell Lung Cancer Who Previously Progressed on Erlotinib. *Clin Cancer Res* **21**, 4321–4326, <https://doi.org/10.1158/1078-0432.CCR-14-3281> (2015).
21. Oki, Y. *et al.* Phase II study of an AKT inhibitor MK2206 in patients with relapsed or refractory lymphoma. *Br J Haematol* **171**, 463–470, <https://doi.org/10.1111/bjh.13603> (2015).
22. Doi, T. *et al.* Phase I pharmacokinetic study of the oral pan-AKT inhibitor MK-2206 in Japanese patients with advanced solid tumors. *Cancer Chemother Pharmacol* **76**, 409–416, <https://doi.org/10.1007/s00280-015-2810-z> (2015).
23. Swami, U., Shah, U. & Goel, S. Eribulin in Cancer Treatment. *Mar Drugs* **13**, 5016–5058, <https://doi.org/10.3390/md13085016> (2015).
24. Demetri, G. D. *et al.* Activity of Eribulin in Patients With Advanced Liposarcoma Demonstrated in a Subgroup Analysis From a Randomized Phase III Study of Eribulin Versus Doxorubicin. *J Clin Oncol* **35**, 3433–3439, <https://doi.org/10.1200/JCO.2016.71.6605> (2017).
25. Sangai, T. *et al.* Biomarkers of response to Akt inhibitor MK-2206 in breast cancer. *Clin Cancer Res* **18**, 5816–5828, <https://doi.org/10.1158/1078-0432.CCR-12-1141> (2012).
26. Almhanna, K. *et al.* MK-2206, an Akt inhibitor, enhances carboplatin/paclitaxel efficacy in gastric cancer cell lines. *Cancer Biol Ther* **14**, 932–936, <https://doi.org/10.4161/cbt.25939> (2013).
27. Rafii, S. *et al.* Higher Risk of Infections with PI3K-AKT-mTOR Pathway Inhibitors in Patients with Advanced Solid Tumors on Phase I Clinical Trials. *Clin Cancer Res* **21**, 1869–1876, <https://doi.org/10.1158/1078-0432.CCR-14-2424> (2015).
28. Narayan, R. S. *et al.* The allosteric AKT inhibitor MK2206 shows a synergistic interaction with chemotherapy and radiotherapy in glioblastoma spheroid cultures. *BMC Cancer* **17**, 204, <https://doi.org/10.1186/s12885-017-3193-9> (2017).
29. Morgillo, F. *et al.* Phosphatidylinositol 3-kinase (PI3K)/AKT axis blockade with taselisib or ipatasertib enhances the efficacy of anti-microtubule drugs in human breast cancer cells. *Oncotarget* **8**, 76479–76491, <https://doi.org/10.18632/oncotarget.20385> (2017).
30. Goto, W. *et al.* Eribulin Promotes Antitumor Immune Responses in Patients with Locally Advanced or Metastatic Breast Cancer. *Anticancer Res* **38**, 2929–2938, <https://doi.org/10.21873/anticancer.12541> (2018).
31. Takada, K. *et al.* Targeted disruption of the BCL9/beta-catenin complex inhibits oncogenic Wnt signaling. *Sci Transl Med* **4**, 148ra117, <https://doi.org/10.1126/scitranslmed.3003808> (2012).
32. Akane, K., Kojima, S., Mak, T. W., Shiku, H. & Suzuki, H. CD8 + CD122 + CD49d^{low} regulatory T cells maintain T-cell homeostasis by killing activated T cells via Fas/FasL-mediated cytotoxicity. *Proc Natl Acad Sci USA* **113**, 2460–2465, <https://doi.org/10.1073/pnas.1525098113> (2016).
33. Agarwal, E. *et al.* Akt inhibitor MK-2206 promotes anti-tumor activity and cell death by modulation of AIF and Ezrin in colorectal cancer. *BMC Cancer* **14**, 145, <https://doi.org/10.1186/1471-2407-14-145> (2014).
34. Arihara, Y. *et al.* Small molecule CP-31398 induces reactive oxygen species-dependent apoptosis in human multiple myeloma. *Oncotarget* **8**, 65889–65899, <https://doi.org/10.18632/oncotarget.19508> (2017).
35. Chou, T. C. Theoretical basis, experimental design, and computerized simulation of synergism and antagonism in drug combination studies. *Pharmacol Rev* **58**, 621–681, <https://doi.org/10.1124/pr.58.3.10> (2006).

Acknowledgements

The authors thank Eisai Inc. (Tokyo, Japan) for providing eribulin, and Yukie Nakamura for her excellent technical assistance.

Author Contributions

All authors have contributed intellectual content to this manuscript as follows: the principal investigators K.T. and N.H. are responsible for the conception and design of the study; N.H., H.N., Y.A., Y.K., T.O., K.M., A.T. and S.K. performed the analysis and interpretation of data; S.I., M.E. and S.S. assessed the studies, extracted the data, and performed the statistical analyses; N.H. and K.T. drafted the manuscript; T.H., M.K. and J.K. performed a critical review; and all of the authors read the manuscript and approved the final version.

Additional Information

Supplementary information accompanies this paper at <https://doi.org/10.1038/s41598-019-42300-z>.

Competing Interests: The authors declare no competing interests.

Publisher's note: Springer Nature remains neutral with regard to jurisdictional claims in published maps and institutional affiliations.



Open Access This article is licensed under a Creative Commons Attribution 4.0 International License, which permits use, sharing, adaptation, distribution and reproduction in any medium or format, as long as you give appropriate credit to the original author(s) and the source, provide a link to the Creative Commons license, and indicate if changes were made. The images or other third party material in this article are included in the article's Creative Commons license, unless indicated otherwise in a credit line to the material. If material is not included in the article's Creative Commons license and your intended use is not permitted by statutory regulation or exceeds the permitted use, you will need to obtain permission directly from the copyright holder. To view a copy of this license, visit <http://creativecommons.org/licenses/by/4.0/>.

© The Author(s) 2019